

Reaction-Based Model Describing Competitive Sorption and Transport of Cd, Zn, and Ni in an Acidic Soil

ANDREAS VOEGELIN,[†]
VIJAY M. VULAVA,[‡] AND
RUBEN KRETZSCHMAR^{*.†}

Institute of Terrestrial Ecology, Swiss Federal Institute of Technology, Grabenstrasse 3, CH-8952 Schlieren, Switzerland, and Savannah River Ecology Lab, University of Georgia, Aiken, South Carolina 29802

Predicting the mobility of heavy metals in soils requires models that accurately describe metal adsorption in the presence of competing cations. They should also be easily adjustable to specific soil materials and applicable in reactive transport codes. In this study, Cd adsorption to an acidic soil material was investigated over a wide concentration range (10^{-8} to 10^{-2} M CdCl₂) in the presence of different background electrolytes (10^{-4} to 10^{-2} M CaCl₂ or MgCl₂ or 0.05 to 0.5 M NaCl). The adsorption experiments were conducted at pH values between 4.6 and 6.5. A reaction-based sorption model was developed using a combination of nonspecific cation exchange reactions and competitive sorption reactions to sites with high affinity for heavy metals. This combined cation exchange/specific sorption (CESS) model accurately described the entire Cd sorption data set. Coupled to a solute transport code, the model accurately predicted Cd breakthrough curves obtained in column transport experiments. The model was further extended to describe competitive sorption and transport of Cd, Zn, and Ni. At pH 4.6, both Zn and Ni exhibited similar sorption and transport behavior as observed for Cd. In all transport experiments conducted under acidic conditions, heavy metal adsorption was shown to be reversible and kinetic effects were negligible within time periods ranging from hours up to four weeks.

Introduction

Pollution of soils with heavy metals can pose serious threats to soil quality and ecosystem health. Metal contaminants in soils may originate from sewage sludge or fertilizer application, smelter and mining emissions, and other human activities. Initially, the chemical nature of the contaminant material may control metal mobility and bioavailability (1). In the long term, however, the chemical speciation of the metal and soil contaminants is altered depending on the metal and soil properties. In acidic soils, metal retention is dominated by adsorption and exchange reactions, and compared to other heavy metals, Cd, Zn, and Ni can be rather mobile (1–3). Major cations such as Ca effectively compete in the adsorption of these metals to cation exchange sites on clay minerals and soil organic matter (4–6). In addition, contaminated

soils typically contain several metal contaminants, which may also compete with each other for sorption sites (7).

Numerous studies have been conducted on Cd, Zn, or Ni sorption to pure soil components such as clay minerals, oxides, or humic substances, and a variety of sorbent-specific models have been developed to describe metal sorption to such materials (8–12). However, predicting metal cation adsorption in soil materials from these results following the component additivity approach is still difficult, because most soils contain a multitude of sorbent phases with different surface properties (13, 14).

Other studies were concerned with heavy metal adsorption to soil materials covering wide ranges in soil properties. The empirical Freundlich equation and various modifications thereof accounting for the effects of soil pH, organic matter content, Ca concentration, and other parameters are used to model the experimental data (2, 4, 15–18). Soil pH and soil organic carbon content were often considered to be the key factors in heavy metal binding (15–19). However, most studies were carried out at background electrolyte concentrations, where nonspecific heavy metal adsorption to cation exchange sites is suppressed, and may hence underestimate the role of cation exchange in metal adsorption.

In transport experiments, competitive sorption of several interacting cations results in complex breakthrough patterns. Therefore, modeling heavy metal transport in soils requires adsorption models that accurately describe the relevant processes. To be applicable in field situations, such models should be simple enough to be adjustable to specific soil materials. While an approach based on sorbent-specific models may be overparametrized and therefore difficult to adjust (13), Freundlich-type equations on the other hand are not applicable, as they cannot correctly describe the coupled adsorption and transport behavior of several cations in multicomponent systems (20).

In this study, we present an extensive new data set on Cd adsorption in an acidic soil material as influenced by major cations and solution pH. A model based on a combination of cation exchange and specific sorption reactions was developed to describe the entire data set. We demonstrate that the model, coupled to a transport code, correctly predicts Cd transport in the presence of varying Ca solution concentrations. The model was also extended to describe coupled Cd/Zn and Cd/Zn/Ni transport experiments.

Experimental Section

Soil Material. Acidic soil material was collected from the B-horizon (15–25 cm sampling depth) of a forested soil in northern Switzerland (Riedhof soil, aquic dystic Eutrochrept, silt loam texture, pH 4.1). The air-dried soil material was sieved to various fractions smaller than 2 mm. For all experiments, the sieve fraction 63–400 μ m was used in order to achieve a homogeneous column packing. This fraction consisted of small soil aggregates containing 37% sand, 47% silt, and 16% clay. The organic carbon content was 9 g/kg organic carbon. From a 0.01 M Ca(NO₃)₂–Mg(NO₃)₂–Ca(NO₃)₂ column exchange experiment at pH 4.6, a pH-dependent effective cation cation exchange capacity (ECEC_{pH}) at pH 4.6 (ECEC_{4.6}) of 0.060 ± 0.002 mol./kg was determined.

Cadmium Adsorption Experiments. Cd adsorption experiments were conducted in Ca, Mg, and Na background electrolyte solutions. The solution concentrations of CdCl₂ ranged from 10^{-8} to 10^{-2} M, while the concentrations of the respective background cations ranged from 10^{-4} to 10^{-2} M for CaCl₂ and MgCl₂ and from 0.05 to 0.5 M for NaCl. The adsorption experiments were carried out using a flow-through

* Corresponding author phone: +41 1 633 6003; fax: +41 1 633 1118; e-mail: kretzschmar@ito.umnw.ethz.ch.

[†] Swiss Federal Institute of Technology.

[‡] University of Georgia.

TABLE 1. Transport Experiments: Column Properties, Flow Conditions, and Composition of the Feed Solution

experiment	column parameters ^a						influent concentrations c_0					pH
	L , cm	d , cm	θ , %	ρ , kg/L	v_p , cm/min	Pe	PV	CdCl ₂ , μ M	ZnCl ₂ , μ M	NiCl ₂ , μ M	CaCl ₂ , ^b mM	
1	9.15	1	58	1.99	1.1	400	35	9.7			10	4.6
2	5.15	1	60	1.99	1.1	200	200	9.8			1	4.6
3	1.85	1	60	2.01	1.1	150	800	9.6			0.101	4.6
4	10.0	1	61	1.95	1.1	400	30	0.98	95		10.1	4.6
5	4.0	1	68	1.87	1.1	100	150	0.99	95		1.01	4.6
6	8.0	2.5	62	1.86	0.41	150	100	28.5	281	29.5	1.03	4.6

^a L = length, d = diameter, θ = porosity, ρ = mass of soil per pore volume, v_p = pore water velocity, Pe = Péclet number, PV = number of pore volumes during which heavy metal containing background electrolyte solution was pumped through the column. ^b Background concentration.

reactor technique (21). Weighed soil samples were placed on cellulose-acetate membrane filters (0.45 μ m) in flow-through reactor cells. All cells were connected to a peristaltic pump, and the soil samples were extensively preconditioned by leaching with 500 mL/g soil 0.5 M CaCl₂, 0.5 M MgCl₂, or 1.0 M NaCl solution at a rate of 3 mL/min. The pH of influent solutions was adjusted by addition of HCl or NaOH. After the prewashing step, when the soil was completely saturated with the respective background cation, the influent electrolyte concentration was reduced to the desired background cation concentration. After equilibrium was reached, the reactors were drained and weighed to determine the amounts of entrapped electrolyte solution. They were then refilled with a solution containing the same background electrolyte plus a known amount of CdCl₂. In this adsorption step, the cell outflow was connected back to the inflow (closed-loop arrangement), and the solution was circulated through the reactor cells for 24 h. After equilibration, cation concentrations were measured in initial and final solutions by atomic absorption (Varian SpectraAA 400 Flame-AAS) and emission (Varian Liberty 200 ICP-AES) spectroscopy. Adsorbed amounts of Cd were calculated from the differences between initial and final solution concentrations and soil weights. The ratio of soil mass to solution volume in each reactor was varied from 50 to 1000 g/L in order to obtain a Cd adsorption between 20% and 80%, allowing reliable estimates of the adsorbed amounts as a function of Cd concentration in solution. A slightly different method was used in the case of Cd adsorption in 10⁻² M CaCl₂ background at pH 5.5: The circulating solution in the closed loop setup was repeatedly spiked with increasing Cd concentrations. Cd, Ca, and pH were monitored online using ion-selective and pH electrodes, respectively. The amount adsorbed was calculated from the difference between the added and the remaining amount of Cd in solution at equilibrium (before next spike). In general, the final pH in the circulating solutions was within initial pH \pm 0.3. Only at the highest Cd concentrations and in low background cation concentrations could the final pH decrease to lower values.

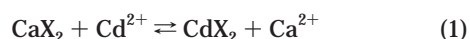
Transport Experiments. Solute transport experiments were conducted in Cd/Ca, Cd/Zn/Ca, and Cd/Zn/Ni/Ca cation systems at pH 4.6 using a packed soil column technique. Chromatographic glass columns (Omni) were uniformly packed with dry soil material and flushed with CO₂ gas to displace the air from the pore space. The columns were then connected to a HPLC pump and preconditioned by passing several hundred pore volumes of 0.5 M CaCl₂ solution adjusted to pH 4.6. Solutions were first passed through a degasser and then through the columns in the upward direction. Due to rapid dissolution of CO₂ gas, complete water saturation was achieved within a few pore volumes. To characterize the hydrodynamic properties of the soil columns, a short (0.1 mL) nitrate pulse was injected and the resulting nitrate breakthrough peak was monitored online using an UV-vis detector set to 220 nm wavelength.

Pore volume, dispersivity, and column Péclet number were determined numerically from the flow rate and the first or second moments of the nitrate breakthrough curves (22). Resulting column parameters and further experimental details are given in Table 1.

For transport experiments, the columns were first leached with the background electrolyte solution, until the column effluent had the same Ca concentration and pH (4.6) as the influent solution. The influent was then switched to a heavy metal containing solution with the same concentration of CaCl₂. After complete heavy metal breakthrough was observed, the influent was switched back to the background electrolyte without heavy metals. Thus, the breakthrough curves corresponding to adsorption and desorption were monitored. The effluents were sampled with a fraction collector, and concentrations of Ca, Cd, Zn, and Ni were measured by atomic absorption spectrometry. The duration of heavy metal inputs and the composition of feed solutions are provided in Table 1.

Cation Exchange/Specific Sorption Model (CESS)

Metal adsorption in soils can include nonspecific (i.e., Coulombic, outer-sphere) interactions, such as cation exchange at negatively charged surfaces of clay minerals and organic matter, as well as specific (i.e., covalent, inner-sphere) binding of metal cations at reactive sites of mineral surfaces and organic matter functional groups (23–25). In our model, nonspecific sorption of heavy metals was described by cation exchange equations. For example, Cd–Ca exchange is written as



where X denotes exchanger sites with charge -1 . The activities of sorbed species were assumed to correspond to the charge equivalent fractions according to the convention of Gaines and Thomas (26). For the binary Cd–Ca system, the following Cd exchange isotherm is obtained

$$q_{\text{CdX}_2} = \frac{1}{2} \text{ECEC}_{\text{pH}} \frac{K_{\text{CdCa}} a_{\text{Cd}^{2+}}}{K_{\text{CdCa}} a_{\text{Cd}^{2+}} + a_{\text{Ca}^{2+}}} \quad (2)$$

where K_{CdCa} is the Gaines–Thomas exchange coefficient, $a_{\text{M}^{2+}}$ is the activity of free metal M, and q_{CdX_2} the amount of Cd adsorbed (in mol/kg). The cation exchange coefficients were assumed to be pH-independent. However, the pH dependence of the ECEC_{pH} was derived from a published regression equation, which relates the soil ECEC_{pH} to clay content, organic carbon content, and soil pH (27). By scaling this equation to the measured $\text{ECEC}_{4.6}$, the following slightly modified equation for ECEC_{pH} (in mol_c/kg) in the Riedhof soil was obtained (for pH 4 to 7):

$$\text{ECEC}_{\text{pH}} = -0.0024 + 0.0135\text{pH} \quad (3)$$

In addition to nonspecific cation exchange, heavy metals can specifically adsorb to high-affinity binding sites located on soil organic matter and oxide or clay mineral surfaces. To account for such reactions, we introduced an additional type of sorption sites using nonelectrostatic site binding equations. The use of electrostatic correction terms would have been questionable due to the complexity of soil materials (13, 14). The specific sorption sites were assumed to have a much greater affinity for heavy metal cations (Cd, Zn, Ni) than for Ca and Mg, respectively. For the adsorption of Cd²⁺ or Ca²⁺, this approach yields the following adsorption equation



where L⁻ denotes free sites and ML⁺ sites occupied by metal M²⁺. The conditional sorption coefficient for eq 4 at experimental pH is then given by

$$K_{M,pH} = \frac{q_{CdL^+}}{q_L a_{Cd^{2+}}} \quad (5)$$

where q_{CdL^+} denotes Cd adsorbed to sites L and q_L is the amount of free sites (both in mol/kg). The pH dependence of metal adsorption to these sites was introduced by assuming that the conditional sorption coefficients vary with pH according to

$$\log K_{M,pH} = \log K_{M,0} + n_M pH \quad (6)$$

where $\log K_{M,pH}$ and $\log K_{M,0}$ are the logarithms of the sorption coefficient at experimental pH and reference pH = 0, respectively. The parameter n_M determines the extent of pH dependence of the respective conditional sorption coefficient. For the binary Cd/Ca system, the following Cd competitive adsorption isotherm is then obtained

$$q_{CdL^+} = L_T \frac{K_{Cd,pH} a_{Cd^{2+}}}{1 + K_{Ca,pH} a_{Ca^{2+}} + K_{Cd,pH} a_{Cd^{2+}}} = L_T \frac{K_{Cd,0} a_H^{-n_{Cd}} a_{Cd^{2+}}}{1 + K_{Ca,0} a_H^{-n_{Ca}} a_{Ca^{2+}} + K_{Cd,0} a_H^{-n_{Cd}} a_{Cd^{2+}}} \quad (7)$$

where L_T is the total concentration of specific sorption sites (in mol/kg). While the left isotherm in eq 7 is based on the conditional sorption coefficients for a given pH, the right expression uses the reference sorption coefficients for pH = 0. This equation could have also been derived by postulating metal adsorption with fractional proton release ($M^{2+} + L^- \rightleftharpoons ML^+ + n_M H^+$ with $K_M = K_{M,0}$). This formulation is often used to account for the observed fractional pH dependence of adsorption reactions on soil organic matter, and the release of protons is either explained by partial hydrolysis of the adsorbing cation or fractional deprotonation of the sorbent (4, 28). The total Cd adsorbed finally is obtained from the sum of Cd adsorbed to the exchange sites (eq 2) and the specific sorption sites (eq 7):

$$q_{Cd} = q_{CdX_2} + q_{CdL^+} \quad (8)$$

Solution speciation was calculated with thermodynamic complex formation constants K_0 derived from conditional constants (29–31) using the Davies equation (32). Complexed species considered (with $\log K_0$ for $M + nL \rightleftharpoons ML_n$ in parentheses) were the following: CaCl⁺ (0.58), MgCl⁺ (0.63), NaCl⁰ (-0.19), CdCl⁺ (1.98), CdCl₂⁰ (2.60), ZnCl⁺ (0.46), ZnCl₂⁰ (0.61), NiCl⁺ (0.40). Transport predictions based on the local equilibrium assumption were calculated with ECOSAT, which numerically solves the convection dispersion equation (33). Input parameters were the column Péclet number (respec-

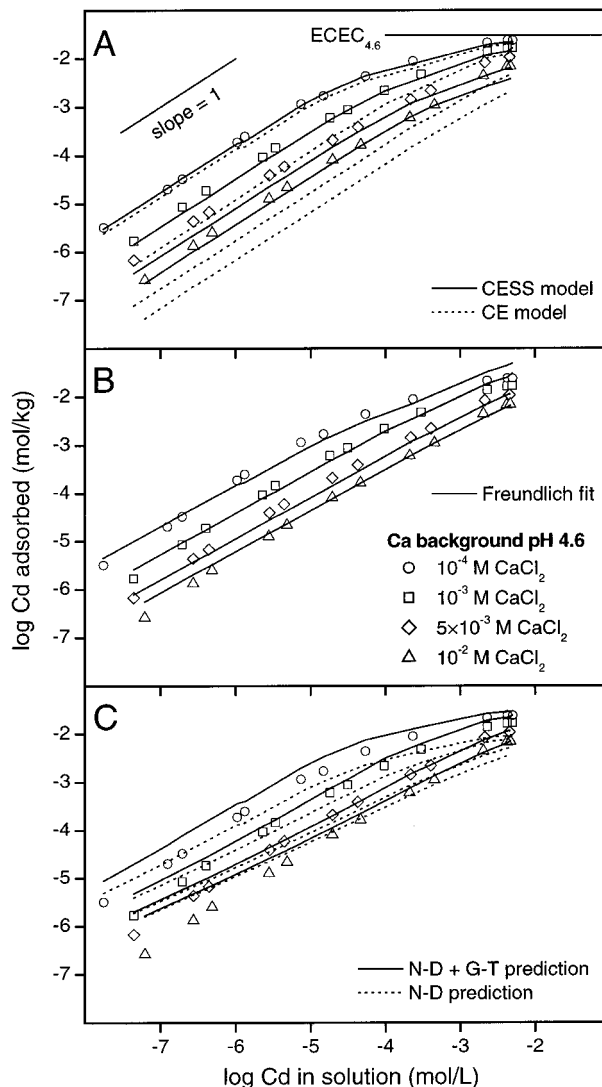


FIGURE 1. Cd adsorption isotherms measured in different CaCl₂ background electrolyte concentrations at pH 4.6 (symbols) described by various modeling approaches. Adsorption increases at decreasing Ca cation concentration. Maximum adsorption is limited by the ECEC_{4.6}. (A) Cation exchange/specific sorption model fit (CESS, solid lines) and cation exchange model fit (CE, dotted lines). (B) Freundlich model fit (solid lines). (C) NICA–Donnan/Gaines–Thomas model prediction (solid lines) and NICA–Donnan part only corresponding to Cd adsorption to soil organic matter (dotted lines). All model calculations are based on measured final cation concentrations.

tively column length, porosity, Darcy velocity, and diffusion coefficient), the bulk density of the soil material, the sorption model parameters, the complex formation constants, and the sequence and composition of feed solutions (Table 1).

Results and Discussion

Cd Adsorption in Ca Background at Constant pH. Experimental adsorption isotherms of Cd in the presence of four different Ca background concentrations at pH 4.6 and corresponding CESS model calculations are presented in Figure 1A. Examining the experimental data first, three main features are evident: (i) the maximum amount of Cd adsorbed is limited by the ECEC_{4.6} of the soil material, (ii) at low Cd concentrations, the isotherms exhibit a constant slope near 1 on a log–log plot, and (iii) the amount of adsorbed Cd generally decreases with increasing Ca concentration. Qualitatively, all of these findings are consistent with Cd adsorption by cation exchange. Hence, as a first approximation, Cd

TABLE 2. Conditional Cation Exchange/Specific Sorption (CESS) Model Parameters for the Riedhof Soil at pH 4.6 and Methods of Parameter Estimation

		Cation Exchange Site ^a	
ECEC _{4.6} (mol _c /kg)	0.060	measured independently	
K _{CdCa}	0.5	fitted to Cd adsorption data in 10 ⁻⁴ M CaCl ₂ /pH 4.6	
K _{MgCa}	0.7	from ref 36	
K _{NaCa}	0.125	from ref 36	
K _{ZnCa}	0.5	estimated as equal to K _{CdCa}	
K _{NiCa}	0.5	estimated as equal to K _{CdCa}	
		Specific Sorption Site ^b	
L _T (mol/kg)	0.002	fitted to Cd adsorption data at pH 4.6	
K _{Cd,4.6}	21000	fitted to Cd adsorption data at pH 4.6	
K _{Ca,4.6}	450	fitted to Cd adsorption data at pH 4.6	
K _{Mg,4.6}	315	estimated: K _{Mg,4.6} = K _{Ca,4.6} K _{MgCa}	
K _{Zn,4.6}	10000	fitted to transport experiments 4 and 5 (at pH 4.6)	
K _{Ni,4.6}	10000	estimated as equal to K _{Zn,4.6}	

^a Based on Gaines–Thomas cation exchange convention, eqs 1–3.

^b Based on nonelectrostatic site binding equations, eqs 4–7.

adsorption was modeled with a Gaines–Thomas cation exchange equation only (eq 1, CE model). While ECEC_{4.6} was determined independently, the value of K_{CdCa} was adjusted to describe Cd adsorption at the lowest Ca concentration, where cation exchange is expected to dominate Cd adsorption. The resulting model calculations show that a pure cation exchange (CE) model can describe Cd adsorption at low Ca concentration but strongly underestimates Cd adsorption at high Ca concentrations (Figure 1A, dashed lines). This suggests that the soil material may contain additional sorption sites with a high Cd affinity (23). Thus, additional competitive binding sites with higher Cd affinity were introduced (eq 4). Additional model parameters are the conditional site binding coefficients (eq 6) and the site concentration. The combined cation exchange/specific sorption (CESS) model returned a greatly improved description of the experimental data over the entire range in Cd and Ca concentrations (Figure 1A, solid lines). Corresponding model parameters are reported in Table 2. The conditional sorption coefficients reflect the high Cd affinity of the specific sorption sites. While cation exchange accounts for most Cd adsorbed at low Ca and/or high Cd concentrations, the specific sorption sites account for Cd adsorption in the presence of high Ca concentrations.

The same adsorption data together with a scaled Freundlich fit is presented in Figure 1B. The modified Freundlich equation $\log(q_{Cd}) = -0.72 + 0.86 \log(a_{Cd^{2+}}) - 0.52 \log(a_{Ca^{2+}})$ with only three adjustable parameters also yields a good description of the experimental data. However, further use of this model for transport calculation is limited for several reasons. As can be seen from the Cd adsorption data in 10⁻⁴ M CaCl₂ background, the model does not account for the adsorption maximum corresponding to the ECEC_{4.6}. It yields a constant isotherm slope of 0.86, which apparently represents a compromise between the experimental slope of 1 at low Cd concentrations and the decreasing slope toward the adsorption maximum. The slight curvature in the plotted Freundlich model calculations at high Cd concentrations results from the measured increase in equilibrium Ca concentration due to Cd–Ca exchange. Finally, the Freundlich model only represents a description of the Cd adsorption data, without assuming any consistent underlying reaction equations with defined stoichiometry. For these reasons, the model cannot be extended to systems with additional cations and cannot describe coupled multicomponent transport patterns involving several interacting cations (20).

Figure 1C shows the experimental data along with model predictions based on a component additivity approach. In

these calculations, Cd sorption to the clay fraction was calculated using the Gaines–Thomas cation exchange equation, and Cd binding to soil organic matter was predicted with the NICA–Donnan model (12, 34). In this prediction, we assumed that 9 g/kg organic carbon corresponds to approximately 7.7 g/kg of humic acid, implying that about 50% of the organic matter content consists of reactive humic acids. Cd, Ca, and H adsorption was calculated with ECOSAT (33) using recently published generic NICA–Donnan parameters for humic acid (35). To account for nonpreferential Cd adsorption on the soil clay fraction, a Gaines–Thomas cation exchange site was introduced in analogy to eq 1 with a K_{CdCa} equal to 1. On the basis of the measured ECEC_{4.6} and of published regression equations for clay and organic carbon contributions to soil ECEC (27), the ECEC of the soil clay fraction at pH 4.6 was estimated as 0.049 mol_c/kg. The calculated contribution of Cd adsorption to humic substances (dashed lines, Figure 1C) indicates that Cd binding to the organic matter fraction plays an important role. The combined model yields a reasonable prediction of the Cd adsorption data (solid lines), considering the uncertainty of the assumptions made. However, to obtain a more accurate description of the Cd adsorption data, further model calibration to the Riedhof soil material would still be necessary. This would again result in an empirical fit to the experimental data, however, with a model approach that has a larger number of adjustable parameters than the CESS model.

Cd Adsorption in Mg and Na Background. In a previous paper, we reported on the competitive sorption of the major cations Ca, Mg, and Na to the same soil material at pH 4.6 (36). The resulting Gaines–Thomas exchange coefficients were K_{MgCa} = 0.70 and K_{NaCa} = 0.125, respectively. In the CESS model, these values were adopted for the cation exchange sites, but the conditional sorption coefficients for Mg and Na to the specific sorption sites had to be estimated. For Mg adsorption, we assumed that the specific sorption sites exhibit the same preference for Ca over Mg as indicated by the Gaines–Thomas Ca–Mg exchange coefficient, K_{MgCa} (Table 2). This seems reasonable, because the adsorption preference for Ca originates mainly from organic matter in soils (37). Adsorption of monovalent Na ions to the specific sorption sites was assumed to be negligible. Panels A and B of Figure 2 show the experimental Cd adsorption isotherms and corresponding model predictions obtained with the pure cation exchange model (dashed lines) and the CESS model (solid lines), respectively. In both types of background electrolyte, the CESS model gave clearly improved predictions of Cd adsorption to the soil material. In the MgCl₂ background electrolyte, the CESS model predicted Cd adsorption quite accurately. In the NaCl background electrolyte, larger deviations are still observed, which may in part be related to the high chloride concentrations in solution, as discussed later.

Cd Adsorption in Ca Background at Variable pH. To account for pH effects on Cd adsorption, the conditional CESS model (Table 2) was extended as described earlier (eqs 3 and 6). The pH dependence of the ECEC_{pH} (eq 3) was adopted from the literature (27). Hence, only the pH dependence of the specific sorption coefficients, i.e., the parameters n_{Cd} and n_{Ca} (eq 6), were adjusted to optimize the description of the Cd adsorption data at variable pH. Figure 2C shows that the extended model yields a good description (solid lines) of Cd adsorption at pH values above 4.6 (open symbols), notably at Ca background concentration levels differing by 2 orders of magnitude. It is interesting to note that, at low Cd concentrations, the effect of increasing pH by ~2 units is comparable to the effect of decreasing the Ca concentration by 2 log units. At high Cd concentrations, however, the decrease in Ca concentration has a larger effect than the increase in pH. This is in agreement with the model assumption that pH mainly affects metal adsorption to the

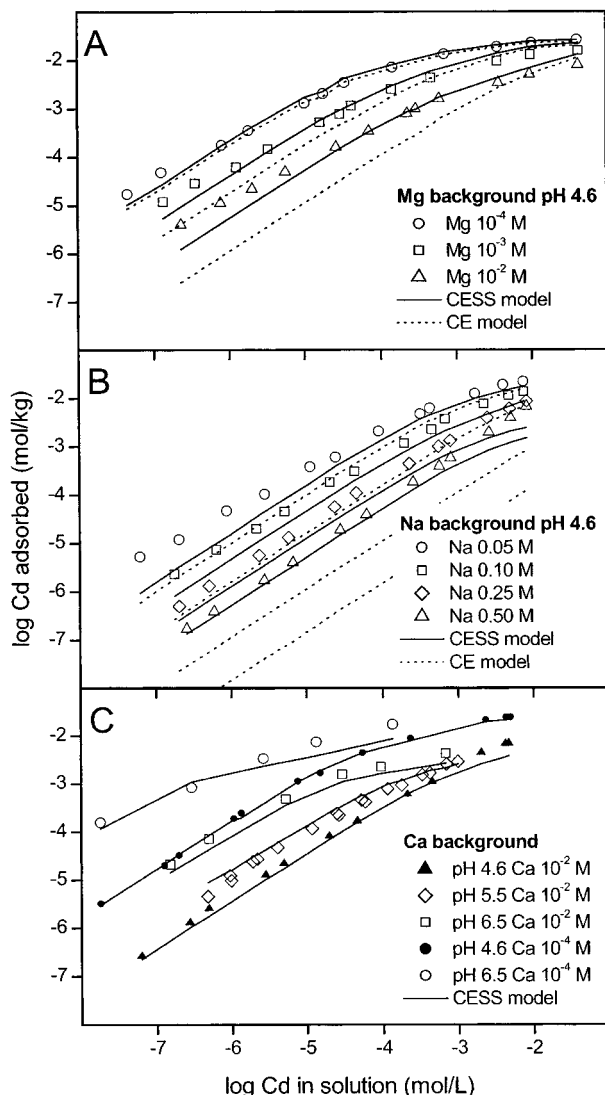


FIGURE 2. Extension of the CESS model to Cd adsorption in (A) Mg and (B) Na background electrolyte solutions at pH 4.6 and (C) to Cd adsorption at variable pH in Ca background electrolyte solutions. CESS model *predictions* (solid lines) for Cd adsorption in Mg and Na background electrolyte (A, B) are clearly improved compared to the CE model (dotted lines). The CESS model could also be *fit* to Cd adsorption at variable pH in Ca background electrolyte (C). All model calculations are based on measured final cation concentrations.

small number of high affinity sites, whereas Ca has a stronger effect on adsorption to the larger number of nonspecific exchange sites. The parameters for the pH-dependent Cd adsorption model in Ca background electrolyte are given in Table 3.

Cd–Ca Transport Experiments. Breakthrough curves of 10^{-3} M Cd in the presence of three different Ca concentrations in the influent (10^{-4} to 10^{-2} M) are presented in Figure 3 (Table 1, experiments 1–3). Decreasing Ca concentration from 10^{-2} to 10^{-4} M resulted in a strong increase of Cd retention. Note that the number of pore volumes is shown on a log scale. The arrows indicate the switch to Cd free influent solutions and subsequent desorption of Cd. The influence of Ca on Cd transport is consistent with the effects on Cd adsorption shown in Figure 1. As expected, the pure cation exchange model (CE, dashed lines) provided a reasonable prediction of Cd transport at low Ca concentration (10^{-4} M), but it strongly underestimated Cd retention at higher Ca levels. In contrast, the CESS model (solid lines) accurately

TABLE 3. Cation Exchange/Specific Sorption (CESS) Model Parameters for Cd Adsorption to the Riedhof Soil at Variable pH in Ca Background Electrolyte and Methods of Parameter Estimation

		Cation Exchange Site ^a	
ECEC _{pH}	(mol _c /kg)	$-0.0024 + 0.0135\text{pH}$	adopted from literature, eq 3
K_{CdCa}		0.5	from Table 2
		Specific Sorption Site ^b	
L_T	(mol/kg)	0.002	from Table 2
n_{Cd}		1.224	fitted to Cd adsorption data with pH > 4.6
$\log K_{\text{Cd},0}$		-1.307	calculated from $K_{\text{Cd},4.6}$ and n_{Cd} , eq 6
n_{Ca}		0.588	fitted to Cd adsorption data with pH > 4.6
$\log K_{\text{Ca},0}$		-0.050	calculated from $K_{\text{Ca},4.6}$ and n_{Ca} , eq 6

^a Based on Gaines–Thomas cation exchange convention, eqs 1–3.
^b Based on nonelectrostatic site binding equations, eqs 4–7.

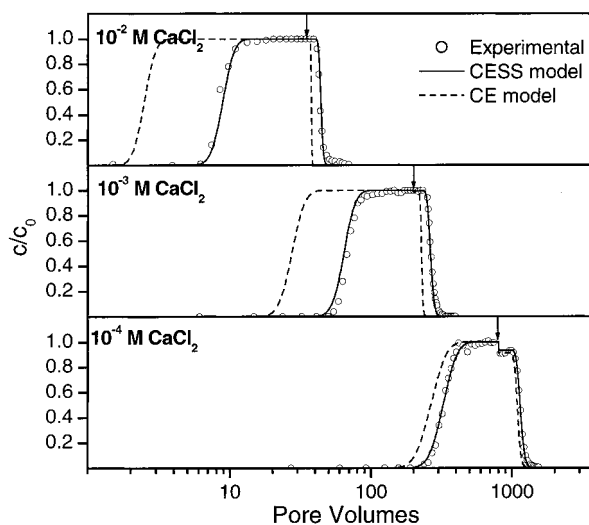


FIGURE 3. Breakthrough curves of Cd in the presence of 10^{-2} , 10^{-3} , and 10^{-4} M CaCl_2 background electrolyte at pH 4.6 (experiments 1–3). The influent solution contained 10^{-5} M CdCl_2 ; arrows indicate the switch back to Cd free influent solutions. Experimental data (symbols) are compared with corresponding model predictions based on a pure cation exchange (CE) model and the cation exchange/specific sorption (CESS) model, respectively.

predicted Cd transport behavior at all three Ca concentrations.

Cd–Zn–Ca Transport Experiments. Cd contamination most often occurs together with other heavy metals, especially with Zn. The average Zn-to-Cd ratio in rock materials is typically around 500:1, and a similar ratio is often observed in contaminated soils (1). More relevant than pure Cd transport experiments may therefore be coupled transport experiments of Cd and Zn. Panels A and B of Figure 4 show the breakthrough of 10^{-6} M Cd in the presence of 10^{-4} M Zn in 10^{-2} and 10^{-3} M CaCl_2 background electrolyte (Table 1, experiments 4 and 5). The addition of Zn resulted in a decrease in Cd retardation by approximately 15–20% when compared to the respective Zn free experiments (data not shown). The mobilizing effect of Zn relative to its concentration is more pronounced than the effect of Ca. Zn is likely to specifically adsorb to the same sites as Cd (38) and hence is a stronger competitor for specific sites than Ca. This demonstrates that a model designed to describe a real multicomponent soil system must include the competitive sorption of several heavy metals. Zn adsorption was incorporated into the model by defining the respective exchange

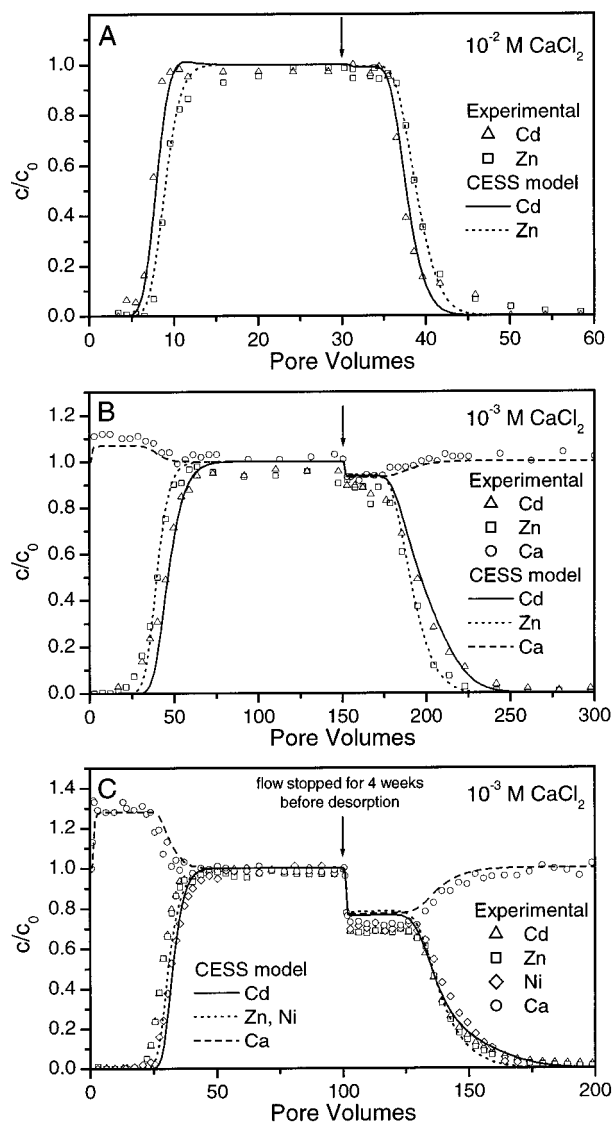


FIGURE 4. Coupled breakthrough curves of Cd, Zn, Ni, and Ca at pH 4.6: (A) 10^{-6} M CdCl₂ and 10^{-4} M ZnCl₂ in 10^{-2} M CaCl₂ background electrolyte solution (experiment 4); (B) 10^{-6} M CdCl₂ and 10^{-4} M ZnCl₂ in 10^{-3} M CaCl₂ background electrolyte solution (experiment 5); and (C) 3×10^{-5} M CdCl₂, 3×10^{-4} M ZnCl₂, and 3×10^{-5} M NiCl₂ in 10^{-3} M CaCl₂ background electrolyte solution (experiment 6). Arrows indicate the switch back to heavy metal free influent solutions. In part C, the flow was stopped for 4 weeks prior to leaching with heavy metal free influent solution. Symbols represent experimental data; lines represent CESS model calculations.

and specific sorption reactions in analogy to Cd. The exchange coefficient K_{ZnCa} was set equal to K_{CdCa} , assuming similar adsorption behavior of Zn and Cd to the nonspecific cation exchange sites. The specific Zn sorption coefficient $K_{Zn,4.6}$ was adjusted to a lower value than $K_{Cd,4.6}$ to obtain an adequate description of Zn breakthrough in 10^{-3} M CaCl₂ electrolyte solution (Figure 4B) occurring slightly ahead of Cd breakthrough. In contrast, at the higher CaCl₂ concentration (Figure 4A), Zn breakthrough occurred slightly after Cd breakthrough. This effect was correctly predicted with the CESS model and can be explained by the greater stability of the CdCl⁺ than of the ZnCl⁺ complex, assuming that metal chloride complexes do not adsorb to the soil material (39).

Cd–Zn–Ni–Ca Transport Experiments. At concentration levels typical for contaminated soils, Ni was reported to exhibit a similar adsorption behavior as Cd or Zn (2, 6). Experimental results and model predictions for the combined

breakthrough of Cd, Zn, and Ni in 10^{-3} M CaCl₂ background electrolyte (Table 1, experiment 6) are presented in Figure 4C. Breakthrough of Cd and Zn occurs simultaneously, while Ni is slightly more retarded. In the model calculation, Ni sorption parameters were set equal to those of Zn. Though the model is slightly off for all three metals, the experiment clearly shows the similar adsorption behavior, notably at acidic conditions and rather high concentration levels.

The Ca concentration plateaus above influent concentration during heavy metal adsorption and below influent Ca concentration during heavy metal desorption clearly indicate ongoing exchange and competitive sorption processes between Ca and Zn, Cd, and Ni. The sharp increase of the Ca effluent concentration at 1 pore volume and the sharp decrease of all cation concentrations 1 pore volume after desorption start result from changes in the influent solution normality. In our experiments, these so-called unretarded normality fronts can be observed where the metal concentrations significantly contribute to total solution normality, i.e., in experiments 3, 5, and 6. (Figures 1 and 4B,C). All these phenomena again give reasons for the application of a model based on exchange and competitive sorption reactions and are correctly described by the CESS model. Considering the two other model approaches discussed earlier, it is apparent that the Freundlich equation is not applicable to such multication systems. The component additivity approach, on the other hand, is rather complex and overparametrized, making it more difficult to adjust the model parameters.

Influence of Anions. Adsorption of stable CdCl⁺ complexes was neglected in the CESS model, which correctly predicted the mobilizing effect of Cl on Cd in comparison to Zn (Figure 4A). This and the results from a limited number of Cd transport and adsorption experiments in Ca(NO₃)₂ background electrolyte solution (not shown) suggest that adsorption of the monovalent CdCl⁺ complex was indeed negligibly weak compared to the adsorption of bivalent metal cations, as observed by other researchers (4, 40). In the case of Cd adsorption in NaCl background electrolytes, notably at very high Cl concentrations (0.05 to 0.5 M), Cd adsorption was underestimated by the CESS model (Figure 2B). This may be due to adsorption of CdCl⁺ complexes. Compared to the effects of competing cations, however, the influence of the background anion is, in any case, of minor importance; and for most practical purposes, neglecting CdCl⁺ adsorption seems to be justified.

Kinetic Effects and Reversibility. Transport calculations based on the local equilibrium assumption correctly described adsorption as well as desorption curves (Figures 3 and 4), suggesting that kinetic effects were not decisive and that adsorption was reversible. These findings were confirmed by further transport experiments where flow rates were varied over 2 orders of magnitude and by repeated adsorption/desorption cycles in the same soil columns (not shown). In experiment 6 (Figure 4C), the flow was stopped for 4 weeks after Cd, Zn, and Ni in the effluent had reached the influent concentration levels, leading to an increase in solution residence time by approximately a factor 2000. When desorption was started, solution pH had increased from pH 4.6 to 5.4, probably due to H–Ca exchange. However, it quickly decreased again and reached the influent pH 4.6 within several pore volumes. All cation concentrations in the effluent were slightly lower than predicted; however, the effect was small and may have been caused by physical processes, e.g., slow diffusion of ions into small pores. Overall we found that, in the presented experiments, kinetic effects were of minor importance and heavy metal adsorption was reversible. It has to be kept in mind, however, that this applies for experiments carried out at rather high heavy metal concentrations typical for contaminated soils ($>10^{-6}$ M), under acidic conditions, and in a soil material with low

organic matter content. More pronounced kinetic effects might occur in soils with higher organic matter contents (41). At higher pH values, greater differences in the sorption behavior of Cd, Ni, and Zn and stronger kinetic effects must be expected. At neutral to basic conditions, slow formation of new solid phases such as hydroxides or layered double hydroxides may cause kinetic effects and immobilization of heavy metals (42–45).

Model Performance. The combined cation exchange/specific sorption (CESS) model approach accurately predicted Cd transport in soil columns and was successfully extended to account for competitive sorption and transport of Zn and Ni. The model is based on stoichiometrically balanced sorption reaction equations, and it can be extended to additional components by adding the respective reaction equations. This allows the description of multicomponent systems based on model parameters derived in simpler, e.g., binary systems. The presented model is conditional for one specific acidic soil material. Nevertheless the general approach presented here should be applicable to other soil materials. Due to the inherent heterogeneity of soils, parameter adjustment will be necessary to achieve an accurate description of competitive metal sorption and transport behavior.

Acknowledgments

We thank Kurt Barmettler for technical support in the laboratory and Stephan Kraemer for helpful comments on an earlier version of the manuscript. Financial support of this research by the Swiss Ministry of Science and Education, in the framework of EU project FAMEST, is gratefully acknowledged.

Literature Cited

- (1) Alloway, B. J. *Heavy Metals in Soils*; Chapman & Hall: London, 1995.
- (2) Buchter, B.; Davidoff, B.; Amacher, M. C.; Hinz, C.; Iskandar, I. K.; Selim, H. M. *Soil Sci.* **1989**, *148*, 370–379.
- (3) Abd-Elfattah, A.; Wada, K. *J. Soil Sci.* **1981**, *32*, 271–283.
- (4) Temminghoff, E. J. M.; van der Zee, S. E. A. T. M.; de Haan, F. A. M. *Eur. J. Soil Sci.* **1995**, *46*, 649–655.
- (5) Christensen, T. H. *Water Air Soil Pollut.* **1984**, *21*, 105–114.
- (6) Wang, W.-Z.; Brusseau, M. L.; Artiola, J. F. *J. Contam. Hydrol.* **1997**, *25*, 325–336.
- (7) Christensen, T. H. *Water Air Soil Pollut.* **1987**, *34*, 293–303.
- (8) Goldberg, S. *Adv. Agron.* **1992**, *47*, 233–329.
- (9) Venema, P.; Hiemstra, T.; van Riemsdijk, W. H. *J. Colloid Interface Sci.* **1996**, *183*, 515–527.
- (10) Venema, P.; Hiemstra, T.; van Riemsdijk, W. H. *J. Colloid Interface Sci.* **1996**, *181*, 45–49.
- (11) Benedetti, M. F.; Milne, C. J.; Kinniburgh, D. G.; van Riemsdijk, W. H.; Koopal, L. K. *Environ. Sci. Technol.* **1995**, *29*, 446–457.
- (12) Kinniburgh, D. G.; Milne, C. J.; Benedetti, M. F.; Pinheiro, J. P.; Filius, J.; Koopal, L. K.; van Riemsdijk, W. H. *Environ. Sci. Technol.* **1996**, *30*, 1687–1698.
- (13) Zachara, J. M.; Westall, J. C. In *Soil Physical Chemistry*; Sparks, D. L., Ed.; CRC Press: Boca Raton, FL, 1998; pp 47–95.
- (14) Davis, J. A.; Coston, D. B.; Fuller, C. C. *Environ. Sci. Technol.* **1998**, *32*, 2820–2828.
- (15) Anderson, P. R.; Christensen, T. H. *J. Soil Sci.* **1988**, *39*, 15–22.

- (16) Boekhold, A. E.; van der Zee, S. E. A. T. M. *Soil Sci.* **1992**, *154*, 105–112.
- (17) Elzinga, E. J.; van Grinsven, J. J. M.; Swartjes, F. A. *Eur. J. Soil Sci.* **1999**, *50*, 139–149.
- (18) Sauve, S.; Hendershot, W.; Allen, H. E. *Environ. Sci. Technol.* **2000**, *34*, 1125–1131.
- (19) Lee, S.-Z.; Allen, H. E.; Huang, C. P.; Sparks, D. L.; Sanders, P. F.; Peijnenburg, W. J. G. M. *Environ. Sci. Technol.* **1996**, *30*, 3418–3424.
- (20) Voegelin, A.; Kretzschmar, R. *J. Contam. Hydrol.* (submitted).
- (21) Grolimund, D.; Borkovec, M.; Federer, P.; Sticher, H. *Environ. Sci. Technol.* **1995**, *29*, 2317–2321.
- (22) Villiermaux, J. In *Percolation Processes: Theory and Applications*; Rodrigues, A. E., Tondeur, D., Eds.; Sijthoff and Noordhoff: Alphen aan den Rijn, 1981; pp 83–140.
- (23) Hendrickson, L. L.; Corey, R. B. *Soil Science* **1981**, *131*, 163–171.
- (24) Sposito, G. *The chemistry of soils*; Oxford University Press: New York, 1989.
- (25) McBride, M. B. *Environmental Chemistry of Soils*; Oxford University Press: New York, 1994.
- (26) Gaines, G. L. J.; Thomas, H. C. *J. Chem. Phys.* **1953**, *21*, 714–718.
- (27) Curtin, D.; Rostad, H. P. W. *Can. J. Soil Sci.* **1997**, *77*, 621–626.
- (28) McBride, M.; Sauvé, S.; Hendershot, W. *Eur. J. Soil Sci.* **1997**, *48*, 337–346.
- (29) Smith, R. M.; Martell, A. E. *Critical Stability Constants*, 4th ed.; Plenum Press: New York, 1976.
- (30) Martell, A. E.; Smith, R. M. *Critical Stability Constants*, 5th ed.; Plenum Press: New York, 1982.
- (31) Smith, R. M.; Martell, A. E. *Critical Stability Constants*, 6th ed.; Plenum Press: New York, 1989.
- (32) Sposito, G. *The Thermodynamics of Soil Solutions*; Oxford University Press: New York, 1981.
- (33) Keizer, M. G.; De Wit, J. C.; Meussen, J. C. L.; Bosma, W. J. P.; Nederlof, M. M.; Venema, P.; Meussen, V. C. S.; van Riemsdijk, W. H.; van der Zee, S. E. A. T. M. *ECOSAT, A computer program for the calculation of speciation in soil–water systems*; Wageningen, The Netherlands, 1993.
- (34) Kinniburgh, D. G.; van Riemsdijk, W. H.; Koopal, L. K.; Borkovec, M.; Benedetti, M. F.; Avena, M. J. *Colloids Surf., A* **1999**, *151*, 147–166.
- (35) Milne, C. J. Measurement and modelling of ion binding by humic substances. Ph.D. Thesis, University of Reading, Reading, 2000.
- (36) Voegelin, A.; Vulava, V. M.; Kuhnén, F.; Kretzschmar, R. *J. Contam. Hydrol.* **2000**, *46*, 319–338.
- (37) Sposito, G.; Fletcher, P. *Soil Sci. Soc. Am. J.* **1985**, *49*, 1160–1163.
- (38) Christensen, T. H. *Water Air Soil Pollut.* **1987**, *34*, 305–314.
- (39) Doner, H. E. *Soil Sci. Soc. Am. J.* **1978**, *42*, 882–885.
- (40) Boekhold, A. E.; Temminghoff, E. J. M.; van der Zee, S. E. A. T. M. *J. Soil Sci.* **1993**, *44*, 85–96.
- (41) Strawn, D. G.; Sparks, D. L. *Soil Sci. Soc. Am. J.* **2000**, *64*, 144–156.
- (42) Roberts, D. R.; Scheidegger, A. M.; Sparks, D. L. *Environ. Sci. Technol.* **1999**, *33*, 3749–3754.
- (43) Thompson, H. A.; Parks, G. A.; Brown, G. E. J. *J. Colloid Interface Sci.* **2000**, *222*, 241–253.
- (44) Ford, R. G.; Sparks, D. L. *Environ. Sci. Technol.* **2000**, *34*, 2479–2483.
- (45) Scheidegger, A. M.; Strawn, D. G.; Lamble, G. M.; Sparks, D. L. *Geochim. Cosmochim. Acta* **1998**, *62*, 2233–2245.

Received for review May 24, 2000. Revised manuscript received January 5, 2001. Accepted January 5, 2001.

ES0001106